

INTRODUCTION

In recent years, the concrete elements of large size are being used owing to the advances made in materials, and improvement in design and construction techniques. One of the problems of increase in size is the evaluation of nominal shear strength. The nominal shear strength of a reinforced concrete beam has been found in experiments to be gradually reduced as the beam depth increases; this is generally regarded as the size effect in shear. In order to estimate the accurate shear strength of large reinforced concrete structures, the experiment for large reinforced concrete beams without shear reinforcement was conducted where the effective depth ranges from 10 cm to 300 cm ⁽¹⁾. On the other hand, the progress of numerical procedures based on the finite element method for reinforced concrete structures in the past twenty years is remarkable and shear behavior of reinforced concrete structures has been studied⁽²⁾.

During the last twenty five years, a considerable amount of researches had been conducted world-wide with the aim of developing behavioral model for reinforced concrete in shear comparable to the rationality and generality of the plane-section theory for flexure. These researches were commenced in the belief that the recent advances in both computational power and behavioral understanding make possible the development of a new generation of design models for reinforced concrete subjected to shear⁽³⁾. The material usually used as reinforcement in concrete is Grade 60 A615 steel rebar. However, newly available high-strength materials could be safer and more cost-effective than the current industry standard. Higher strength steel such as A1035 offers not only an increase in strength but also corrosion resistance. As a result, most design code provisions use empirical models developed based on simplified rules of mechanics and/or regression analyses of experimental data. The number of experimental observations used then for developing such models was often limited. These deterministic models exhibit uncertain biases and errors that prevent accurate predictions over a wide range of input parameter values. This uncertainty is due to imperfect descriptions of shear transfer mechanism, missing parameters, and insufficient amount of the test data⁽⁴⁾.

In this study, finite element analyses, which were performed using the ANSYS software, were used to investigate shear behavior of large size beams reinforced with high-strength steel. To validate the present finite element model, comparisons were made with experimental results of previous researchers.

OBJECTIVE

Currently, there is no general agreement on a theory describing the shear behavior of large size reinforced concrete members reinforced with high-strength steel flexural reinforcement. The objective of the research reported herein was to develop recommendations for the theoretical analysis of reinforced concrete beams reinforced with high-strength steel that could be used by practicing engineers.

FINITE ELEMENT MODEL

For this study, finite element analyses, which were performed using the ANSYS software ⁽⁶⁾, were used to investigate shear behavior of large size beams reinforced with normal and high-strength steel as a flexural reinforcement, with different concrete compressive strength and different loading locations.

Eight reinforced concrete beams with different material properties and boundary conditions were modeled without web reinforcement. The loading arrangement, geometrical properties and reinforcement distribution of the analyzed beams are shown in Fig.(1). All beams are subjected to concentrated load acting at midspan. Only the longitudinal reinforcement has been considered. Concrete modulus of elasticity is calculated from $E_c = 4700 \sqrt{f_c}$ ⁽⁷⁾ and concrete cracking stress or rupture module is taken as $f_r = 0.62\lambda \sqrt{f_c}$ for normal weight concrete, $\lambda = 1$ ⁽⁷⁾, while the Poisson's ratio for concrete is considered as $\nu_c = 0.2$. Shear transfer coefficient β_t which represents conditions of the crack face ranges from 0.0 to 1.0, with 0.0 representing a smooth crack (complete loss of shear transfer) and 1.0 representing a rough crack (no loss of shear transfer) ⁽⁶⁾. The important shear transfer mechanisms include (1) the shear in the uncracked compression zone, (2) the dowel action of the longitudinal reinforcement, (3) the interface shear transfer due to the aggregate interlocks or the surface roughness of the cracks, and (4) the residual tensile stresses across the cracks. The shear transfer coefficient used in present study varied between 0.3 and 0.4 because these values showed the best representation of the model and gave results very close to the practical results. Details of the analyzed beams are listed in Table 1.

A 3D element, SOLID65 ⁽⁶⁾, is used to model the concrete in ANSYS. The solid element has eight nodes with three degrees of freedom at each node, translations in the nodal x , y , and z directions. The element is capable of plastic deformation, and cracking in three

orthogonal directions. The concrete is assumed to behave as a homogeneous and initially isotropic material. The multilinear isotropic representation for compressive uniaxial stress-strain relationship for concrete model are used in the present study ⁽⁸⁾. Link8 element ⁽⁶⁾ was used to model steel reinforcement. The steel for the finite element models is assumed to be an elastic-perfectly plastic material while strain hardening is ignored and steel assumed to be identical in tension and compression for both normal and high-strength steel. A Poisson's ratio of $0.3^{(8)}$ is used for the steel reinforcement. The steel reinforcing was connected between nodes of each adjacent concrete solid element, so the two materials shared the same nodes, therefore, a perfect bond between the concrete and steel reinforcement was considered.

In the finite element models, each load is distributed over a small area as for the experimental beams. A 25 mm thick and 250 mm length steel plate, modeled using SOLID45 elements ⁽⁶⁾, is implemented at the support and loading locations in order to avoid stress concentration problems. This provides a more even stress distribution over the support and loading areas. An elastic modulus equal to 200000 N/mm^2 and Poisson's ratio of $0.3^{(8)}$ are used for the steel plates. The steel plates are assumed to be linear elastic materials.

By taking advantage of the symmetry of the beams, a quarter of the full size beams tested by previous researchers ⁽⁵⁾ is used for modeling with proper boundary conditions. The finite element mesh, boundary condition and loading regions of the beam are shown in Fig.(2).

VALIDATION OF FINITE ELEMENT MODEL

The goal of the comparison of the finite element model results with the experimental results is to ensure that the elements, material properties, real constants and convergence criteria are adequate to express the behavior response of the member. The results obtained by the numerical finite element model for six beams (B1 to B6) are compared with the experimental results described in previous research ⁽⁵⁾.

LOAD DEFLECTION CURVES

Midspan deflection values have been plotted at different loading stage up to failure load using finite element model. Fig.(3) and Table (2) show a comparison of the values of midspan deflection between the numerical and experimental results. As seen in Fig.(3), the general behavior of finite element results agree well with the experimental results for the six

beams (B1 to B6). Table 2 shows that the average value of the ratio of the predicted load at first crack to the corresponding load observed in the experiment was found to be 94%. The average value of the ratio of the predicted load at ultimate to the corresponding load observed in the experiment was found to be 93%. The average value of the ratio of the predicted deflection at ultimate to the corresponding deflection observed in the experiment was found to be 90%. That indicates that, the ANSYS model predicted the load and deflection at various stages, namely, at cracking and at ultimate quite accurately.

CRACK PATTERN

Figure (4) show that the cracks predicted using the finite element model was found to be in good agreement with the experimental observation. The ANSYS model predicted cracking of concrete at the ultimate load, which was indicated by large deformation at the node. ANSYS program displays circles at locations of cracking or crushing in concrete elements. Cracking is shown with a circle outline in the plane of the crack, and crushing is shown with an octahedron outline. The first crack at an integration point is shown with a red circle outline, the second crack with a green outline, and the third crack with a blue outline ^[6]. The comparison of the crack pattern predicted to that observed in the experimental results indicated that the ANSYS model predicts the zones of critical cracks quite accurately.

RESULTS AND DISCUSSIONS

The effectiveness of the analytical model in simulating the structural behavior of beam schemes was validated by comparison the numerical results with experimental results in previous research section, in this section finite element model will be used to investigate the effect of the yield strength of flexural reinforcement and the concrete compressive strength on the beams behavior.

LOAD-DEFLECTION BEHAVIOR

The mid-span deflection values for six beams with a/d equal to 1.9 are calculated and plotted as shown in Fig.(5). The six beams are divided into three groups each group consist of a pair of beams the odd beam reinforced longitudinally with normal strength steel while the even beams reinforced with high strength steel, each group have a different value of concrete the even beams reinforced with high strength steel, each group have a different value of

concrete compressive strength (beams B7 and B8 having $f'_c = 32 \text{ N/mm}^2$, beams B3 and B4 having $f'_c = 38 \text{ N/mm}^2$, and beams B5 and B6 having $f'_c = 51 \text{ N/mm}^2$). All beams appeared to display linear behavior to the cracking load point and from that point to first yield of the steel reinforcement. After yielding of the reinforcement began, a large increase in deflection was noticed, while the applied load changed little, this behavior continued until failure was happened. Figure (5) shows that the ultimate applied load increased with use of high strength steel and concrete. The use of high strength steel inhibit the tension failure in the tie and exhibit the compression failure in the strut, therefore; the concrete compressive strength is highly influenced the beam shear strength and the use of high strength steel reinforcement must be accomplished by using high strength concrete to reach to the ultimate strength of the two materials.

DUCTILITY

As seen in Fig.(5) the beam reinforced with high-strength steel show preferable higher ductility at failure than the same beam that reinforced with conventional steel reinforcement. This behavior is due to the high steel strain and smaller area of reinforcement used in high strength steel beam. The values of steel tensile strains at the mid span section for the analyzed beams are shown in Table (3). The overall ductility for all beams are decreased with use of high strength concrete, that decrease is coming from the fact that using high strength concrete allow the beam to resist more loads before the crushing of diagonal strut occur.

MODE OF FAILURE

The results of analysis show that the failure of beams reinforced with conventional steel reinforcement was sudden and show relatively little cracking. While the beams reinforced with high-strength steel show high ductile behavior and large number of cracking. For beams reinforced with conventional steel reinforcement when the tension reinforcement began to yield, flexural-shear cracks began forming in the flexural region of the beam. All cracks continued to grow while the direction of their propagation started to lean towards the load point at approximately from 60° to 90° angles as shown in figure 3. For beams reinforced with high-strength steel reinforcement when the tension reinforcement began to yield, shear and flexural-shear cracks began forming in the shear region of the beam. All cracks continued to grow while the direction of their travel started to lean towards the load

and support points at approximately 45° angles. This continued until the cracks reached approximately 90% of the beam depth and failure occurred.

CONCLUSIONS

From the predicted previously results, namely, loads, deflections and cracking behavior using the model the following conclusions can draw

- The presented finite element model is capable of producing results in good agreement with previous published test results and it can be confidently used in design and analysis situations.
- The use of high-strength steel flexure reinforcement improves the post cracking tensile stiffness of the concrete.
- The shear strength of large size concrete beams reinforced with high-strength steel was significantly higher than that of the beams reinforced with conventional steel reinforcement.
- The use of high-strength steel flexure reinforcement gives a less brittle behavior of the reinforced beams.
- The high yield strength of high-strength steel inhibit the tension failure in the tie and exhibit the compression failure in the strut, therefore; the high concrete compressive strength and high yield strength of flexural steel reinforcement do highly influence the beam shear strength and must be used together.

REFERENCES

1. Mizuhito IGURO, Toshiyuki SHIOYA, Yoichi NOJIRI and Hikaru AKIYAMA, (1985) "Experimental Studies on Shear Strength of Large Reinforced Concrete Beams under Uniformly Distributed Load", Concrete Library of JSCE No.5, pp137.154.
2. Okamura, H. and Maekawa, K., (1991) "Nonlinear Analysis and Constitutive Models of Reinforced Concrete", Gihoudou-Shuppan ISBN : 978-4-7655-1506-1.
3. Evan C. Bentz, (2000) "Sectional Analysis of Reinforced Concrete Members", PhD thesis, Department of civil engineering University of Toronto.
4. Junho Song, Won-Hee Kang, Kang Su Kim and Sungmoon Jung (2010), " Probabilistic shear strength models for reinforced concrete beams without shear reinforcement", Structural Engineering and Mechanics, Vol. 34, No. 1, pp 15-38

5. Tarek K. Hassan, Hatem M. Seliem, Hazim Dwairi, Sami H. Rizkalla, and Paul Zia(2008) "Shear Behavior of Large Concrete Beams Reinforced with High-Strength Steel", ACI Structural Journal, V. 105, No. 2, MS No. S-2006-398.R1
6. ANSYS Manual, Version (10.0).
7. ACI 318m-08, American Concrete Institute,(2008) Building Code Requirements for Reinforced Concrete, American Concrete Institute, Farmington Hills, Michigan.
8. Amer M. Ibrahim and Mohammed Sh. Mahmood (2009), "Finite Element Modeling of Reinforced Concrete Beams Strengthened With FRP Laminates", European Journal of Scientific Research, ISSN 1450-216X Vol.30, No.4, pp.526-541.

NOMENCLATURE

a	Shear span	(mm)
d	Effective beam depth	(mm)
E_c	Concrete elastic modulus	(N/mm ²)
E_s	Steel elastic modulus	(N/mm ²)
f'_c	Ultimate uniaxial compressive strength	(N/mm ²)
f_r	Concrete modulus of rupture	(N/mm ²)
f_y	Steel reinforcement yield strength	(N/mm ²)
ν_c	Concrete Poisson's ratio	
ν_s	Steel Poisson's ratio	
β_t	Shear transfer coefficient	
λ	Modification factor reflecting the reduced mechanical properties of lightweight concrete, all relative to normal weight concrete of the same compressive strength	

Table(1): Summary of beams details⁽⁵⁾.

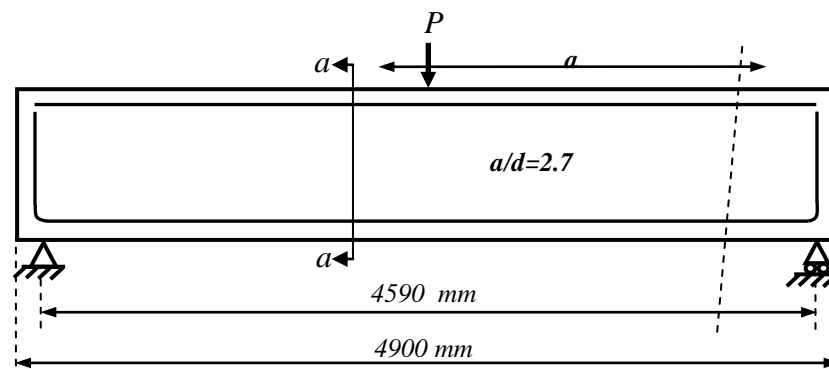
	B1	B2	B3	B4	B5	B6
Shear span to depth ratio a/d	2.7	2.7	1.9	1.9	1.9	1.9
Concrete compressive strength, N/mm^2 (f_c)	32	32	38	38	51	51
Steel reinforcement yield strength, N/mm^2 (f_y)	420	827	420	827	420	827
Steel modulus of elasticity, N/mm^2 (E_s) $\times 10^3$	200	200	200	200	200	200
Top reinforcement ratio, %	0.72	0.44	0.72	0.44	0.72	0.44
Bottom reinforcement ratio, %	0.36	0.22	0.36	0.22	0.36	0.22

Table(2): Comparison of numerical and experimental result.

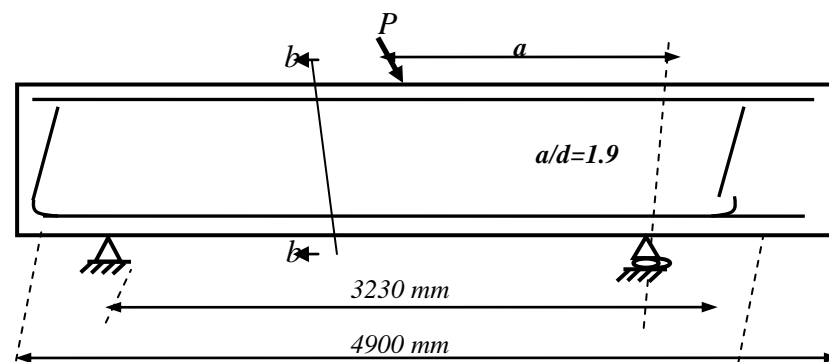
		B1	B2	B3	B4	B5	B6
First cracking load (kN)	Numerical	445	445	670	670	670	670
	Experimental ⁽⁵⁾	470	470	700	700	710	710
Failure load (kN)	Numerical	552	638	753	1364	871	1560
	Experimental ⁽⁵⁾	600	680	830	1430	910	1610
Deflection (mm)	Numerical	10	20	7	17	5	15
	Experimental ⁽⁵⁾	11	22	8	18	5.5	17

Table3: Values of steel tensile strains at the mid span section.

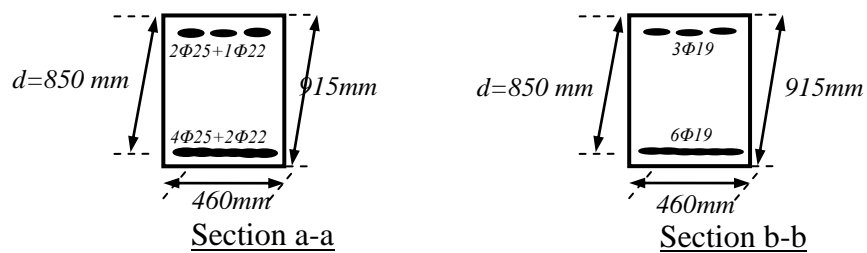
	B7	B8	B3	B4	B5	B6
steel tensile strains ϵ (mm/mm)	0.019	0.053	0.015	0.049	0.013	0.048



a. Dimension and reinforcement of B1 and B2.

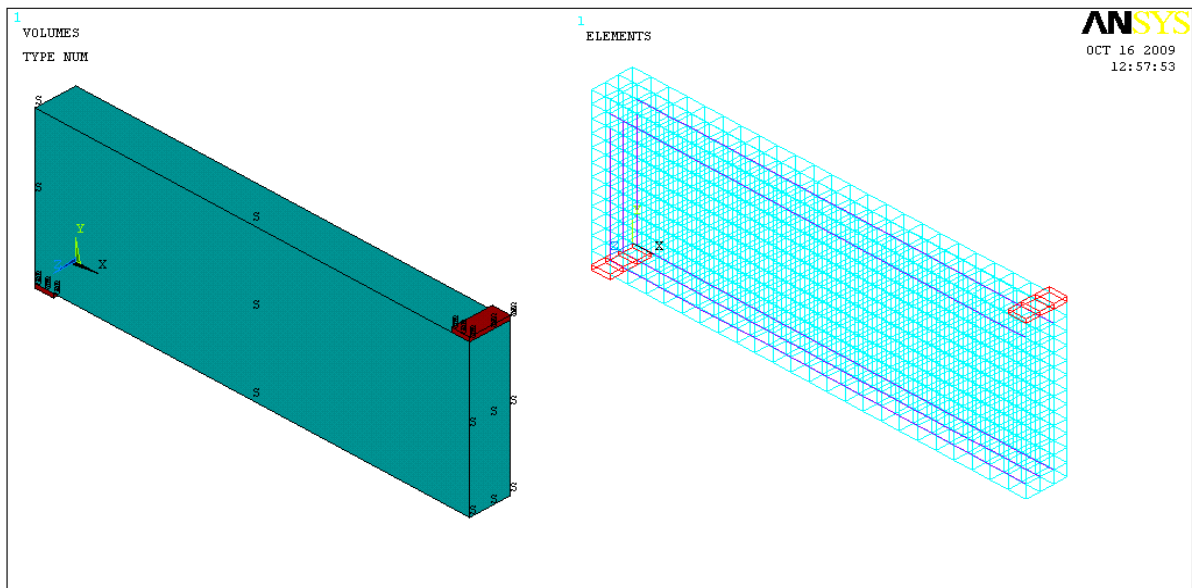


a. Dimension and reinforcement of B3, B4, B5, B6, B7 and B8.

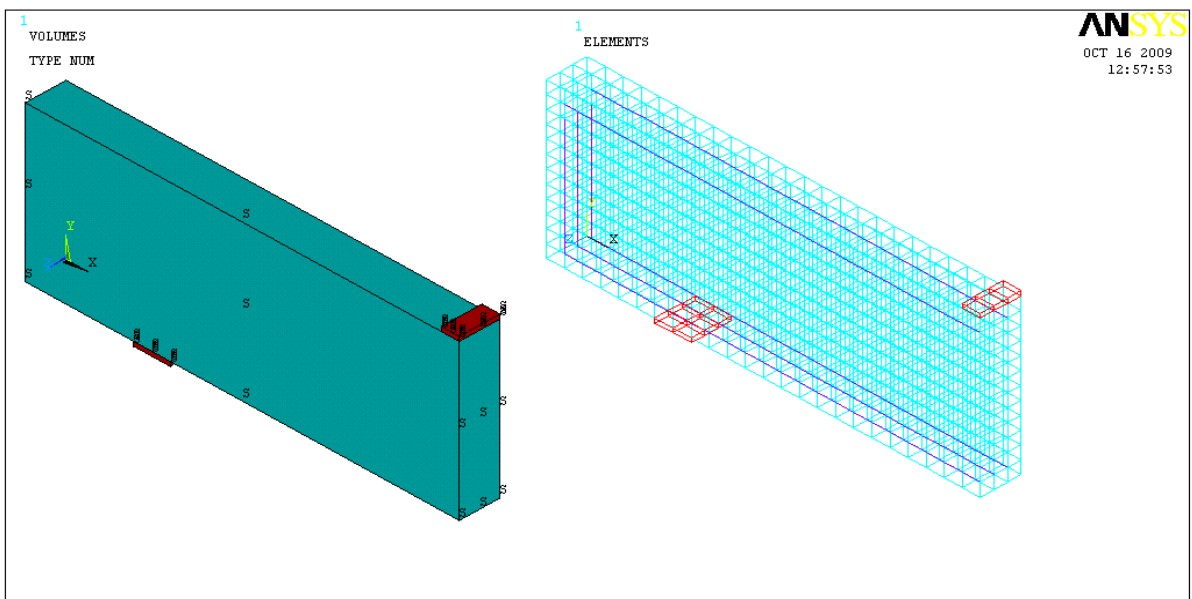


Beams reinforced with conventional Beams reinforced with high-strength
c. Beams cross-sections and reinforcement.

Fig.(1): Loading arrangement and geometrical properties of analyzed beams ⁽⁵⁾.

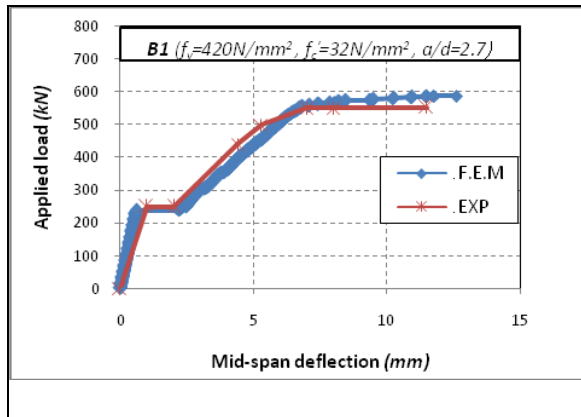


a. Finite element modeling for B1& B2

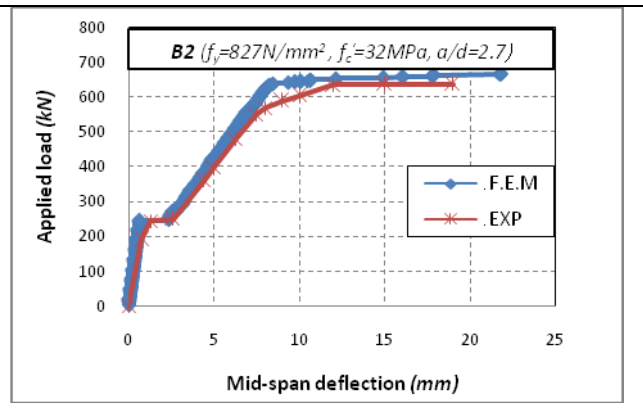


b. Finite element modeling for B3, B4, B5& B6.

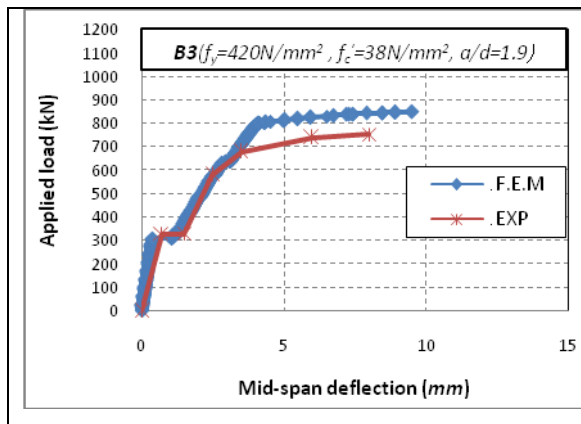
Fig.(2): Finite element mesh, boundary condition and loading regions for a quarter beam model of all beams.



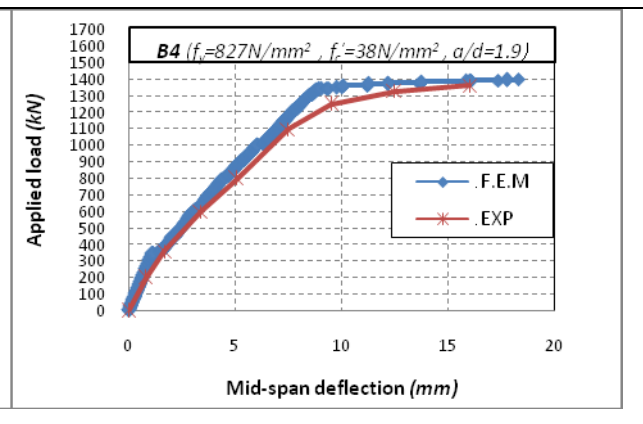
a. Load deflection curve for beam B1.



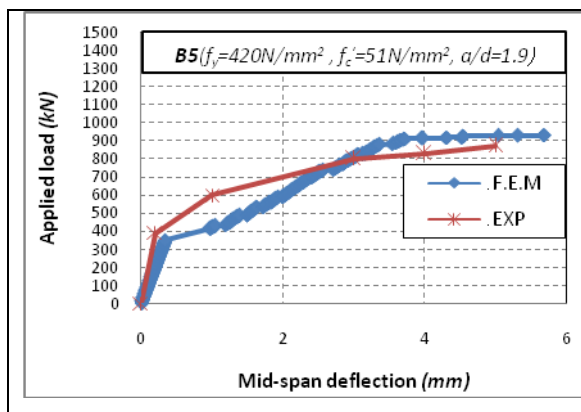
b. Load deflection curve for beam B2.



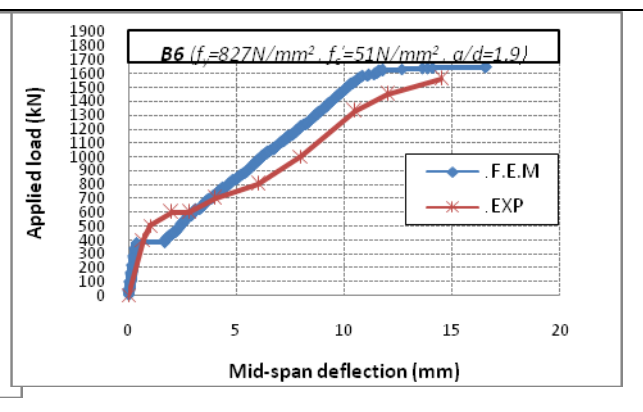
c. Load deflection curve for beam B3.



d. Load deflection curve for beam B4.

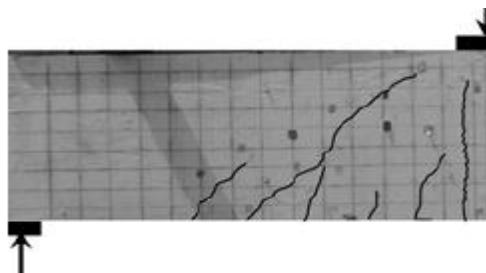


e. Load deflection curve for beam B5.

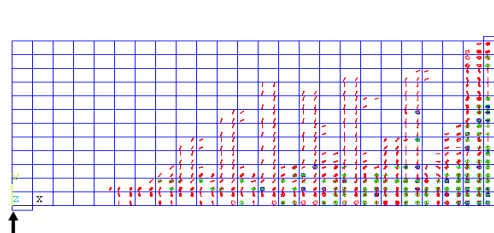


f. Load deflection curve for beam B6.

Fig.(3): Validation of load deflection curves.

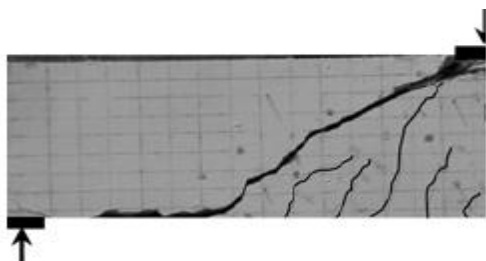


Exp⁽⁵⁾.

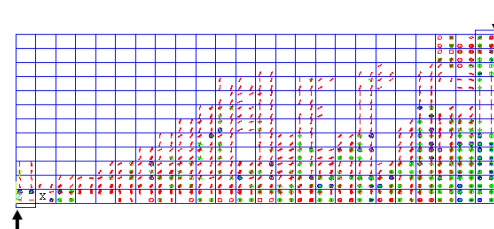


F.E.M.

a. Crack pattern for beam B1.

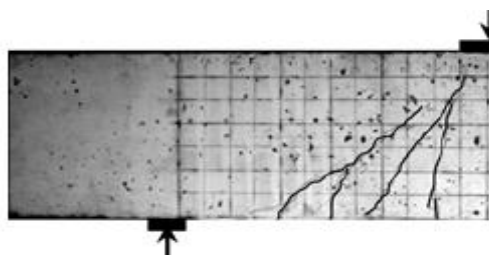


Exp⁽⁵⁾.

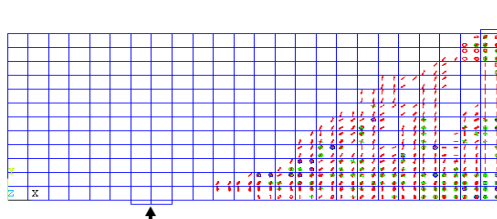


F.E.M.

b. Crack pattern for beam B2.



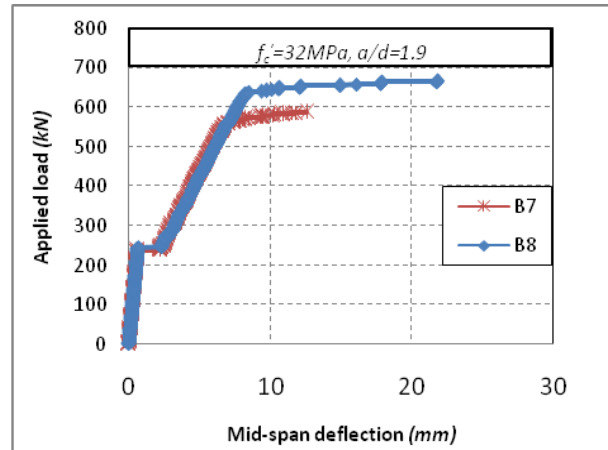
Exp⁽⁵⁾.



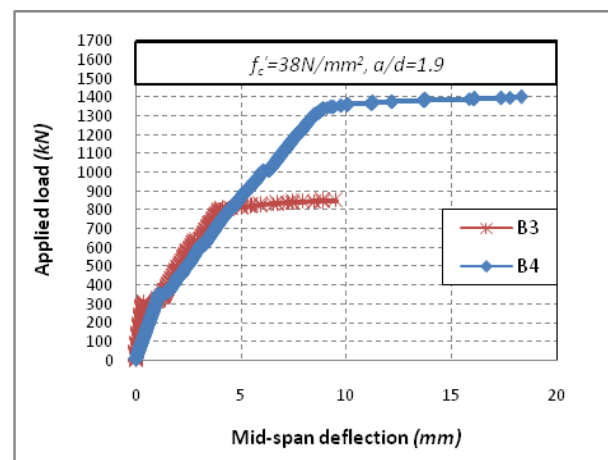
F.E.M.

c. Crack pattern for beam B5.

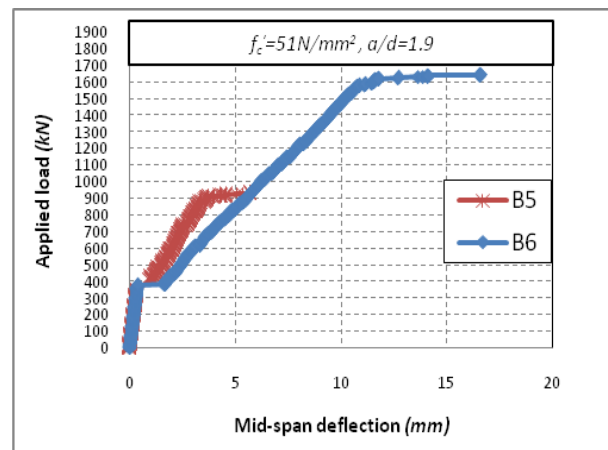
Fig.(4): Validation of Crack pattern.



a. Load deflection curves for B7 and B8



b. Load deflection curves for B3 and B4



c. Load deflection curves for B5 and B6

Fig.(5): Load deflection curves.

التحليل بالعناصر المحددة للأعقاب الخرسانية المسلحة الكبيرة الحجم والمنقوصة المقاومة للقص

محمد شهاب محمود

مساعد مدرس

كلية الهندسة . جامعة ديالى

الخلاصة

يعتبر فشل القص للأعقاب الخرسانية المسلحة ظاهرة كسر معقدة جداً وفي الوقت الحاضر لا توجد معالجة رياضية لهذا الموضوع بشكل محدد. ومع ذلك، فإن النمذجة المفصلة لآلية الكسر ليست ضرورية لإعطاء الشكل العام لتأثير الحجم. هذا البحث يثبت التفاصيل لإستعمال التحليل بالعناصر المحددة بإستخدام برنامج "ANSYS" لثمانية أعقاب خرسانية مسلحة كبيرة الحجم. تم تحليل الأعقاب بدون استخدام حديد تسليح القص لغرض تقييم مقاومة قوة القص الإسمية للخرسانة. المتغيرات الرئيسية التي تضمنتها الدراسة هي النسبة بين بعد نقطة تأثير الحمل المركز من المسند a والعمق المؤثر للعتب d (a/d)، مقاومة الانضغاط للخرسانة f_c' ، ونوع (حديد تسليح تقليدي أو عالي المقاومة) وكمية حديد التسليح الطولي. تم تمثيل الخرسانة بإستخدام "SOLID65" وهو عنصر ثلاثي الأبعاد مؤلف من ثمانية نقاط، والذي يكون قادر على تمثيل سلوك التصدع والسحق للمواد الهشة. حديد التسليح تم تمثيله بإستخدام "LINK8" وهو عنصر مؤلف من نقطتين. تم إجراء مقارنة بين نتائج تحليل العناصر المحددة، الأحمال، الأود وسلوك التصدع مع النتائج التجريبية المتوفرة وقد ظهر تقارب جيد بين النتائج العددية والنتائج التجريبية. النتائج أظهرت بأن إستعمال حديد تسليح عالي المقاومة يحسن من مقاومة الخرسانة للقص وتصدعات الشد للخرسانة.

الكلمات الدلالية: أعقاب خرسانية مسلحة كبيرة الحجم ؛ طريقة العناصر المحددة؛ حديد تسليح عالي المقاومة.